Appl. Phys B 61, 391–399 (1995)

Applied Physics B Lasers and Optics

Large-scale collisional energy transfer in laser-pumped metastable Ca atoms: Excitation of resonance states of Ca II

M.A. Khan, M.A. Gondal, M.H. Rais

Laser Research Section, Energy Resources Division, Research Institute, King Fahd University of Petroleum & Minerals, Dhahran 31261, Saudi Arabia
(Fax: + 966-3/860-4281, E-mail: RSIS2OC@saupm00.bitnet)

Received: 23 June 1994/Accepted: 26 January 1995

Abstract. We report the first experimental observation of the excitation of the $4p\,^2P_{3/2,1/2}$ resonance states of Ca II (located at 74 720.4 and 74 497.5 cm^{-1} above the ground state of Ca I) following pulsed-laser pumping of the $4s^2\,^1S_0$–$4s4p\,^3P_1$ intercombination transition of Ca I ($E_{ex} = 15\,210\ cm^{-1}$). Large scale collisional transfer of energy between the laser-excited atoms is believed to be responsible for this. This is possibly because sufficient time is available (τ_{rad} of the $4s4p\,^3P_1$ state is approximately 350 μs) for collisions to build such a high level of excitation. Some interesting additional features of the fluorescence spectra of the laser-pumped Ca vapor, such as temperature dependence of the fluorescence intensities and evolution in time of some selected states, are also presented.

PACS: 31.70.Hq; 52.25. – b; 34.50.Fa; 32.70. – n

Resonant laser pumping can prepare a large population of atoms in a specific atomic state. In the case of a metastable state, the long radiative lifetime allows the collisional processes to play a dominant role in the reappropriation of energy stored in the atomic state as the system regains a steady state following the pulsed excitation [1–4]. Two of the remarkable consequences are the rapid collisional ionization of the laser-excited atoms [2–4] and quasi-continuous laser action [5, 6]. Among the numerous possible collision processes, the superelastic transfer of the energy of some of the excited atoms to free electrons followed by very rapid electron collisional excitation and ionization of excited and unexcited atoms, is by far the most effective channel of energy transfer [7, 8]. It is to be noted that even before the laser excitation, some free electrons will be present in the vapor due to thermionic emission from metallic surfaces maintained at high temperatures in order to obtain adequate vapor pressure [9, 10]. The higher mobility of electrons together with the possibility of virtually unrestricted amount of energy transfer to and from the free electrons (as opposed to the required matching of energy differences between quantized states in atom–atom and atom–molecule collisions) make this process particularly important. In the specific case of Ca vapor under study here, these processes read as:

$$\text{Ca}\ 4s4p\,^3P_1 + \text{e} \Leftrightarrow \text{Ca}\ 4s^2\,(^1S_0) + \text{e}^*, \tag{1a}$$

$$\text{Ca}\ 4s4p\,^3P_J + \text{e}^* \Leftrightarrow \text{Ca}\ nlml' + \text{e} + \Delta E, \tag{1b}$$

$$\text{Ca}\ nlml' + \text{e}^* \Leftrightarrow \text{Ca}^+(4s\,^2S_{1/2}) + 2\text{e} + \Delta E, \tag{1c}$$

where e* represents an electron with high kinetic energy, Ca $nlml'$ represents a highly excited atom, ΔE is the energy defect, and $Ca^+(4s\,^2S_{1/2})$ is the ground state of Ca II.

In the case of collisions between excited atoms, energy pooling collisions [11–16], associative ionization [17, 18], and Penning ionization [19, 20] can also have high rate coefficients, and can make a significant contribution in the energy transfer chain. However, associative ionization and Penning ionization have not been investigated in any significant detail in the case of Ca. On the other hand, energy pooling collisions have been reported in two previous papers [11, 21].

The present paper reports the first experimental observation of the excitation of the resonance states viz $4p\,^2P_{3/2,1/2}$ of Ca II following pulsed-laser pumping of the $4s^2\,^1S_0$–$4s4p\,^3P_1$ transition of Ca I (Fig. 1). To the best of our information, this constitutes the largest collisional transfer of energy noted in such experiments. Furthermore, the temperature and density dependence of fluorescence intensities of some selected transitions of Ca I and the rate of growth of population in various excited states are investigated. This provides some insights into the dynamics of various collision processes.

1 Experimental details

The experiments were conducted in a vapor cell which has been described in previous publications [2–5, 22]. Briefly, a cylindrical column of Ca vapor 80 mm in length and 25 mm in diameter with vapor density ranging between 1.7×10^{15} and $1.94 \times 10^{16}\ cm^{-3}$ (oven temperature between 725 and 875°C) was irradiated with a laser beam

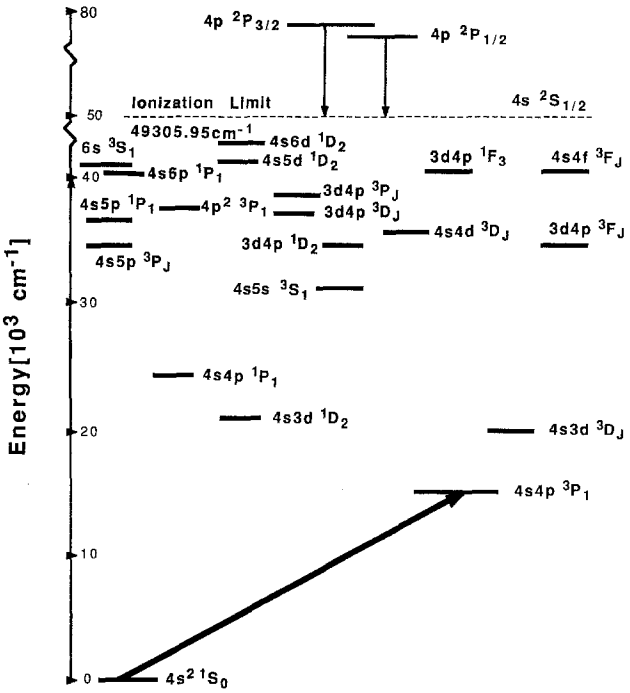

Fig. 1. A partial energy level diagram of Ca showing the laser-pumped transition and other excited states involved in the collisional energy transfer. The $4p\,^2P$ states of Ca II observed in these experiments are also shown

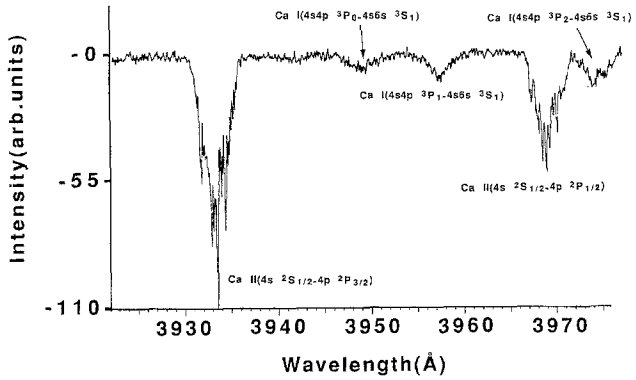

Fig. 2. A typical spectrum of the $4p\,^2P_{3/2,1/2}$–$4s\,^2S_{1/2}$ transitions of Ca II at 3933.66 and 3968.47 Å. Some $4s6s\,^3S_1$–$4s4p\,^3P_1$ transitions of Ca I also appear in this region, but are rather weak

Table 1. Intensities of the observed spectral lines of Ca II emitted by Ca vapor pumped on the $4s^2\,^1S_0$–$4s4p\,^3P_1$ transition of Ca I

Transition	Wavelength [Å]	Intensity[a]
$4s\,^2S_{1/2}$–$4p\,^2P_{3/2}$	3933.663	13.70
$4s\,^2S_{1/2}$–$4p\,^2P_{1/2}$	3968.468	6.90

[a] See text for details

tuned to the $4s^2\,^1S_0$–$4s4p\,^3P_1$ transition at 6572.78 Å. Argon was used as a buffer gas in order to restrict the diffusion of hot vapor towards the optical windows. We also note that the presence of a buffer gas causes a rapid mixing of atomic population within the Ca $4s4p\,^3P_J$ multiplet [4, 23]. Once excited, the truly metastable $4s4p\,^3P_{2,0}$ states also participate in collisional energy transfer mechanisms.

The laser system consisted of a Nd:YAG laser (2nd harmonic) pumping a dye laser employing DCM dye dissolved in methanol. The unfocused laser beam was collimated to approximately 5 mm diameter as it passed through the vapor. Typical laser power was 6×10^4 W cm^{-2} in 10 ns pulses at 20 Hz repetition rate. Time-integrated as well as time-resolved spectral emission from the laser-pumped vapor was recorded using a scanning monochromator (Spex 1870B) and a thermoelectrically cooled photomultiplier (Thorne EMI 9558B). The signals were recorded by a boxcar averager and signal processor (EG&G models 4421 and 4402). Up to 20 pulses were averaged for each data point on the record.

2 Results and discussion

An atom in an excited state de-excites through spontaneous radiative decay or through collisional "quenching"; *or*, it can be further excited and ionized through absorption of additional energy, e.g., in collisions with energetic electrons or other excited atoms. The experimental conditions, like temperature and density, significantly influence the rates of various collisional energy transfer mechanisms. On the other hand, the long radiative lifetime of an excited state may permit the upward collisional processes to meaningfully compete or, in some cases, to even surpass the radiative decay downwards. If the collisions lead to ionization of the atom, recombination will also occur subsequently where the free electron is captured by the ion either directly into the ground state or in a cascade through various excited states. A study of the emitted radiation can provide some important information about various possible radiative and collisional processes, which is the subject of the present paper.

2.1 Excitation of Ca II transitions

Indeed, the most significant result in the present study is the observation of fluorescence due to the ionic transitions $4p\,^2P_{3/2}$–$4s\,^2S_{1/2}$ at 3933.66 Å and the $4p\,^2P_{1/2}$–$4s\,^2S_{1/2}$ at 3968.47 Å. Figure 2 shows a typical spectral record in the 3922–3976 Å region. Here, the oven temperature was 835°C with 640 mbar Ar pressure. Some $4s6s\,^3S$–$4s4p\,^3P$ transitions of Ca I also appear in this region but they are rather weak. Note that the intensities appear negative because of the photomultiplier signal. The measured intensities of the two transitions of Ca II under the experimental conditions discussed above are listed in Table 1. These have been corrected for the response of the photomultiplier at different wavelengths using the data supplied by the manufacturer, and are calculated with reference to the intensity of the $4s4p\,^1P_1$–$4s^2\,^1S_0$ transition of Ca I at 4226.73 Å arbitrarily fixed at 10000.

Figure 3 shows a record of the spectral emission due to the $4p\,^2P_{3/2}$–$4s\,^2S_{1/2}$ transition of Ca II as the dye laser is scanned over the wavelength region around 6572.78 Å

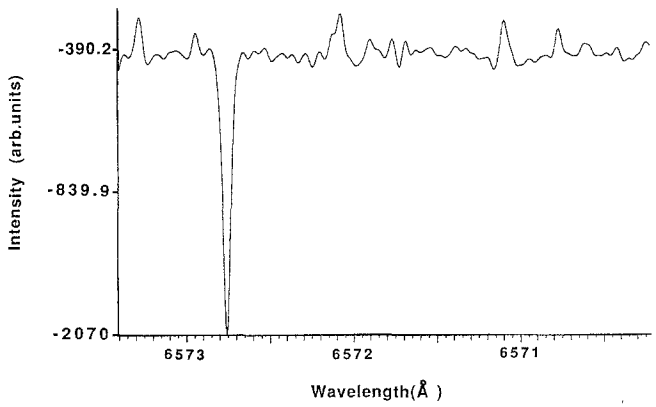

Fig. 3. A record of the spectral emission from the $4p\,^2P_{3/2}$–$4s\,^2S_{1/2}$ transition of Ca II at 3933.66 Å as the laser is scanned around 6572.78 Å covering the wavelength region of the $4s^2\,^1S_0$–$4s4p\,^3P_1$ transition of Ca I

corresponding to the pumped transition $4s^2\,^1S_0$–$4s4p\,^3P_1$ of Ca I. Here the monochromator was fixed at 3933.66 Å corresponding to the peak of Ca II transition.

We recorded the emission spectra at even higher oven temperatures viz 900°C and searched for the $4d$–$4p$ and the $5s$–$4p$ transitions of Ca II in the 3150–3200 and 3720–3770 Å regions but these did not appear in our spectra. On the other hand, the $3d\,^2D_{5/2,3/2}$ states of Ca II are metastable and no emission from these states could be recorded. Thus, the highest level excited in these experiments was $4p\,^2P_{3/2}$ of Ca II.

Excitation of the $4p\,^2P_{3/2,1/2}$ ionic states is possible after the transfer of the cumulative energy of 5 laser photons to a ground state Ca I atom. Equivalently, collisional transfer of the cumulative energy of four laser-excited atoms ($4s4p\,^3P_1$ state) to a fifth laser-excited atom should also create these states. In an attempt to study possible nonlinear multiphoton absorptions, the dependence of the fluorescence intensities I of the emitted lines at different laser powers P was investigated. However, the $\log(I)$ vs $\log(P)$ plot yielded a slope of 1.4 instead of 5 required for a five-photon nonlinear excitation which ruled out multiphoton absorptions. This is understandable otherwise also since the laser power density was rather low because no focusing optics were used as noted earlier. This suggests that collisional energy transfer is the only possible mechanism for excitation of these ionic states.

In an attempt to further investigate the excitation of the $4p$ states of Ca II, we recorded the time-resolved fluorescence from these states. Figure 4a shows an example of the time-resolved emission from the $4p\,^2P_{3/2}$ state at 3933.66 Å when the oven temperature was 875 °C. In order to obtain a good estimate of the rise and fall times of the signal, a 50 Ω termination was used here instead of the 1 MΩ termination elsewhere. The population in the $4p\,^2P_{3/2}$ state apparently reaches a peak in about 4–5 μs (Fig. 4b) while the collapse of its population occurs in about 10 μs. This may be contrasted with our measurements for the high-lying Ca I states in the same experiment where the collapse of population occurred in about 20–30 μs. We further note that the lifetime of the $4p\,^2P$

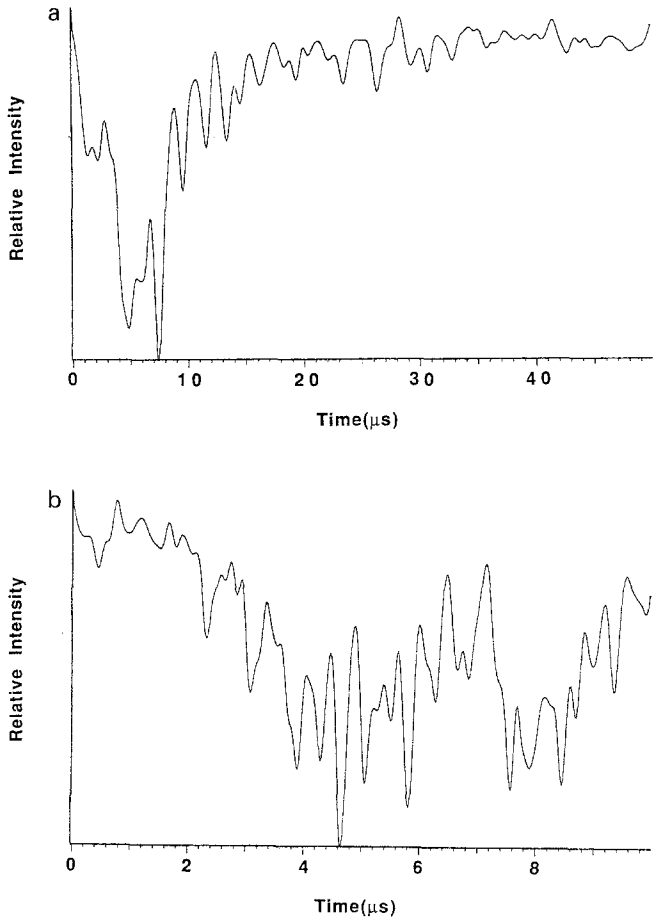

Fig. 4. a Time-resolved emission from the $4p\,^2P_{3/2}$–$4s\,^2S_{1/2}$ transition of Ca II at 3933.66 Å; **b** Rise time to the peak of spectral emission for the transition in 5(a)

states is only about 6 ns [24]. This also suggests the collisional rather than the multiphoton origin of the excitation. The point to be noted here is that a substantial level of population is needed in the laser-prepared metastable state ($4s4p\,^3P_1$) to cause the collisional excitation of a state of such a high energy in the first place. Furthermore, a substantial level of population must be maintained in the laser-pumped state ($4s4p\,^3P_1$) for a certain length of time in order to continue to feed the high energy states through a chain of inelastic collisions.

A one-step collisional transfer of such a large amount of energy looks rather improbable. We believe that essentially a step-wise transfer of energy takes place. This is confirmed by the presence of Ca atoms in several high lying "intermediate states" (located between the laser-pumped state and the $4p$ product states of Ca II) such as $4s4p\,^1P$, $4s5s\,^3S$; $4s4d\,^3D$; $4s5p\,^{1,3}P$; $3d4p(^{1,3}D, {}^3F)$ and $4p^2\,^3P$ in large numbers as witnessed by their intense emission spectra [25].

2.1.1 Possible collision channels. Collisional ionization of laser-pumped hot and dense vapors is indeed a well-known phenomenon [2–4, 7–8, 26]. In addition, the experiments of Le Gouet et al. [27] on laser-pumped alkali vapors have clearly proved that collisions supported by

Table 2. Some illustrative examples of possible energy pooling collisions

System	Product state	Atomic states of possible collision partners		Energy defect $\Delta E = E_p - (E_1 + E_2)$ [cm^{-1}]
		1	2	
Ca I	$4s4p\,^1P_1$	$4s4p\,^3P_1$	$4s4p\,^3P_1$	− 6768
	$4s5s\,^3S_1$	$4s4p\,^3P_1$	$4s4p\,^3P_1$	+ 1120
	$3d4p\,^3F_4$	$4s4p\,^3P_1$	$4s3d\,^3D_3$	+ 316
	$4s4d\,^3D_3$	$4s4p\,^3P_1$	$4s4p\,^1P_1$	− 1105
	$4p3d\,^3D_3$	$4s4p\,^3P_1$	$4s4p\,^1P_1$	− 603
Ca II	$4p\,^2P_{3/2}$	$4s4d\,^3D_3$	$4s4d\,^3D_3$	− 795
	$4p\,^2P_{3/2}$	$4p3d\,^3D_3$	$4p3d\,^3D_3$	− 1798
	$4p\,^2P_{3/2}$	$4p3d\,^3D_3$	$4p3d\,^3F_4$	+ 564
	$4p\,^2P_{1/2}$	$4s4d\,^3D_3$	$4s4d\,^3D_3$	− 1018
	$4p\,^2P_{1/2}$	$4p3d\,^3D_3$	$4p3d\,^3D_3$	− 2021
	$4p\,^2P_{1/2}$	$4p3d\,^3D_3$	$4p3d\,^3F_4$	+ 341

superelastically heated electrons are mainly responsible for the large-scale ionization. In fact, they observed a whole range of energies for free electrons *extracted* from the atoms excited to many different states. Furthermore, experiments in our laboratory [2–4] have confirmed that collisional ionization of laser-pumped Ca vapor occurs rapidly. However, the chain of collision processes presented in (1a–c) are just a few examples among several possibilities. The point to be emphasized here is that there is no logical reason to believe that in the sequence of events shown in (1a–c), further excitation of $Ca^+\ 4s(^2S_{1/2})$ will not occur especially if the pool of laser-excited atoms has a long lifetime and the process of superelastic *extraction* of energy by free electrons and its subsequent reappropriation can continue for a long time. However, the energy losses through radiation and convective diffusion will have to remain fairly small.

Thus, a process like

$$Ca^+\ 4s(^2S_{1/2})) + e^{**} \Rightarrow Ca^+\ 4p(^2P_{3/2}) + e + \Delta E \qquad (2)$$

looks quite probable. Here, the electron e** should have enough kinetic energy to cause this excitation. Indeed, a very large number of other possibilities can be imagined. For example, it is also possible to directly excite a Ca I atom in a high Rydberg state through a collision with a more energetic electron.

$$Ca\,m'l'n'l'' + e^{**} \Rightarrow Ca^+\ 4p(^2P_{3/2}) + 2e + \Delta E. \qquad (3)$$

The same result may also be achieved through energy pooling collisions of excited atoms such as $2 \times 4s4d\,^3D$ or $2 \times 3d4p\,^3D$ or $(3d4p\,^3D + 3d4p\,^3F)$ atoms which are possible at least from a purely intuitive point of view. In particular, we may consider the following processes:

$$Ca\ 3d4p(^3D_3) + Ca\ 3d4p(^3F_4) \Leftrightarrow Ca^+\ 4p(^2P_{3/2}) + Ca\ 4s^2(^1S_0) + e + \Delta E, \qquad (4a)$$

or,

$$Ca\ 4s4d(^3D_3) + Ca\ 4s4d(^3D_3) \Leftrightarrow Ca^+\ 4p(^2P_{3/2}) + Ca\ 4s^2(^1S_0) + e + \Delta E. \qquad (4b)$$

The energy defect ΔE is only about 564 cm^{-1} for the process (4a), and about 795 cm^{-1} for the process (4b) which are within the thermal energies of the colliding atoms. However, the rate coefficients of such atom–atom (A–A) processes remain rather low. In fact, the energy transfer may be more readily and rapidly negotiated through an initial transfer to a free electron involving a superelastic *extraction* of energy from a highly excited atom (e–A collision) and its subsequent transfer to another excited atom involving a further superelastic e**–A collision similar to the process (3) above. It may be remarked that the best way to differentiate between the e–A and A–A collisions is to incorporate an *in situ* energy analysis of the free electrons which can be correlated with the possible intermediate states [27]. This again is a formidable task which we have not undertaken so far. However, in our discussion of the A–A collisions, we shall assume that the e–A collisions are inherently included.

Table 2 lists some possible A–A collisions between identical as well as nonidentical excited atoms which might yield the product states of interest to the excitation ladder producing the $4p\,^2P$ states of Ca II. The product states and the energy defects are also listed in the same table. E_p, E_1, and E_2 are, respectively, the energies of the product state, and of the two colliding atoms. The level energies used (but not listed here) were taken from Sugar and Corliss [28]. As an explanation of this table, the first row will be read as

$$Ca\ 4s4p(^3P_1) + Ca\ 4s4p(^3P_1) \Leftrightarrow Ca\ 4s4p(^1P_1) + Ca\ 4s^2(^1S_0) + \Delta E, \qquad (5)$$

where ΔE is about 6768 cm^{-1}. We may note that these are only some illustrative examples. The actual list of such processes may be very long. For example, the pooling of atoms in the $4s4p(^3P_{2,0})$ states which is also expected to be significant, is not listed in Table 2. Similarly, as noted in our previous investigations [29], the $4s3d(^3D)$ states are also formed in large numbers, although these are not listed as product states. The emission from the $4s3d\,^3D$–$4s4p\,^3P$ transitions is in the infrared region and was not recorded in the present studies.

The relative rates for most of the processes listed in Table 2 are unknown. However, an estimate of the rate coefficient for the formation of Ca $4s4p(^1P_1)$ state through energy pooling of two Ca $4s4p(^3P_1)$ states was presented by Malin and Benard [21] to be 10^{-11}–10^{-12} $cm^3\,s^{-1}$.

We may further note that following the creation of some intermediate states (in large numbers) in the first

step as displayed in the first two rows of Table 2, A–A collisions involving these intermediate states may also occur. For instance, collisions involving identical atoms like

$$2 \times \text{Ca } 4s3d(^3D_J) \Leftrightarrow \text{Ca } n^*l^*m^*l^* + \text{Ca } 4s^2(^1S_0) + \Delta E, \quad (6)$$

or,

$$2 \times \text{Ca } 4s4p(^1P_1) \Leftrightarrow \text{Ca } n^*l^*m^*l^* + \text{Ca } 4s^2(^1S_0) + \Delta E, \quad (7)$$

as well as non-identical atoms like

$$\text{Ca } 4s4p(^3P_J) + \text{Ca } 4s3d(^3D_J) \Leftrightarrow \text{Ca } n^*l^*m^*l^* + \text{Ca } 4s^2(^1S_0) + \Delta E, \quad (8)$$

or,

$$\text{Ca } 4s4p(^1P_1) + \text{Ca } 4s3d(^3D_J) \Leftrightarrow \text{Ca } n^*l^*m^*l^* + \text{Ca } 4s^2(^1S_0) + \Delta E, \quad (9)$$

thereby producing some highly excited states Ca n^*l^* m^*l^*, seem quite probable. In this case, atomic states like $4s4d\,^3D$, $3d4p(^{1,3}D, ^3F)$ may be formed. Similarly, we may have A–A collisions involving atoms in the $4p3d(^{1,3}D, ^3F)$ and $4s4d(^3D)$ states (Table 2) yielding the $4p$ states of Ca II as in (4a) and (4b) above.

The above-mentioned possibilities could not be confirmed in simple experiments involving time-integrated studies of fluorescence where only the final "product" state is observed irrespective of the intermediate states or channels of its excitation. However, we have also carried out time-resolved studies of the fluorescence from some selected intermediate states in order to obtain some information of interest. But, the ionic spectra remained rather weak and the required resolution was not available. Furthermore, the temperature and density dependence of the ionic spectra could not be investigated over a wider range because of the same reason.

2.2 *Spectra of high lying states of Ca I*

We recorded the emission spectra from the laser-pumped Ca vapor over a wide spectral range (3600–9000 Å) by scanning the monochromator [25]. Typical examples of the observed spectra of some $4s5d(^3D)$–$4s4p(^3P)$ transitions in the 3620–3674 Å region, and the $3d4p(^1D, ^3F)$–$4s3d(^3D)$ transitions in the 6435–6488 Å region are shown in Fig. 5a, b respectively. Indeed, some interesting information can be obtained from the recorded spectra. For example, as noted earlier, the transitions originating from the $4s4p(^1P)$, $4s5s(^3S)$; $4s4d(^3D)$; $4s5p(^{1,3}P)$; $3d4p(^{1,3}D, ^3F)$ and $4p^2(^3P)$ states were particularly strong suggesting that these are the important intermediate states involving in the energy transfer chain. On the other hand, the spectra of states higher than $4s6p$ were absent. This was obviously due to their large orbital radii and the strong collision effects which possibly caused their immediate ionization [30].

It was further noted that the spectra from the triplet states are generally much stronger compared with the singlet states except for the case of $4s4p(^1P)$ state which

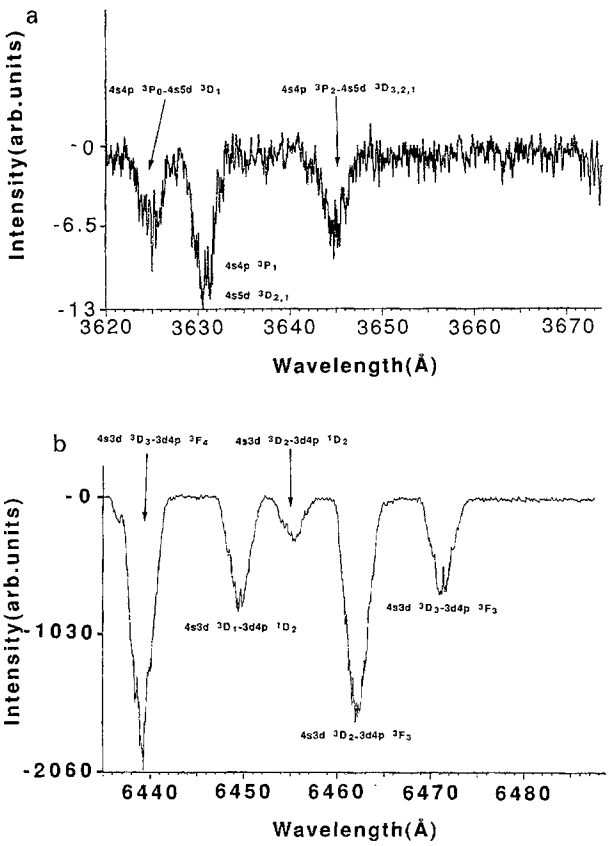

Fig. 5a, b. Typical records of spectral emission from laser-pumped Ca vapor: **a** in the 3620–3674 Å region showing some $4s5d(^3D)$–$4s4p(^3P)$ transitions; and **b** in the 6435–6488 Å showing some $3d4p(^1D, ^3F)$–$4s3d(^3D)$ transitions. Here the oven temperature was 835 °C with 640 mbar Ar pressure

emits one of the strongest lines at 4226.73 Å. In fact, the emission from the $4s4p(^3P_1)$–$4s^2(^1S_0)$ transition is slightly weaker compared with the $4s4p(^1P_1)$–$4s^2(^1S_0)$ transition because of the much smaller oscillator strength [24].

We have estimated the electron temperature in the laser-pumped Ca vapor from the relative intensities of various transitions terminating at the same lower level *viz* $4s3d(^3D_2)$, in this case. A value of about 0.39 eV was obtained which seems to be reasonable for such experiments [26].

Several other features of the emission spectra were also investigated. These include the influence of base temperature and vapor density on the spectral intensities as well as the rate of growth of atomic population in various high lying excited states.

2.2.1 Study of energy pooling collisions. We recorded the emission spectra at different temperatures in the 725–850 °C range, and systematically monitored the fluorescence intensities of some selected transitions such as the $4s4p(^1P_1)$–$4s^2(^1S_0)$ at 4226.73 Å, $4s5s(^3S_1)$–$4s4p(^3P_2)$ at 6162.17 Å, and $4s4d(^3D_3)$–$4s4p(^3P_2)$ at 4454.78 Å. The main aim was to look for the evidence of energy pooling collisions.

The intensity I of a particular transition is related to the population N of the upper state of the transition

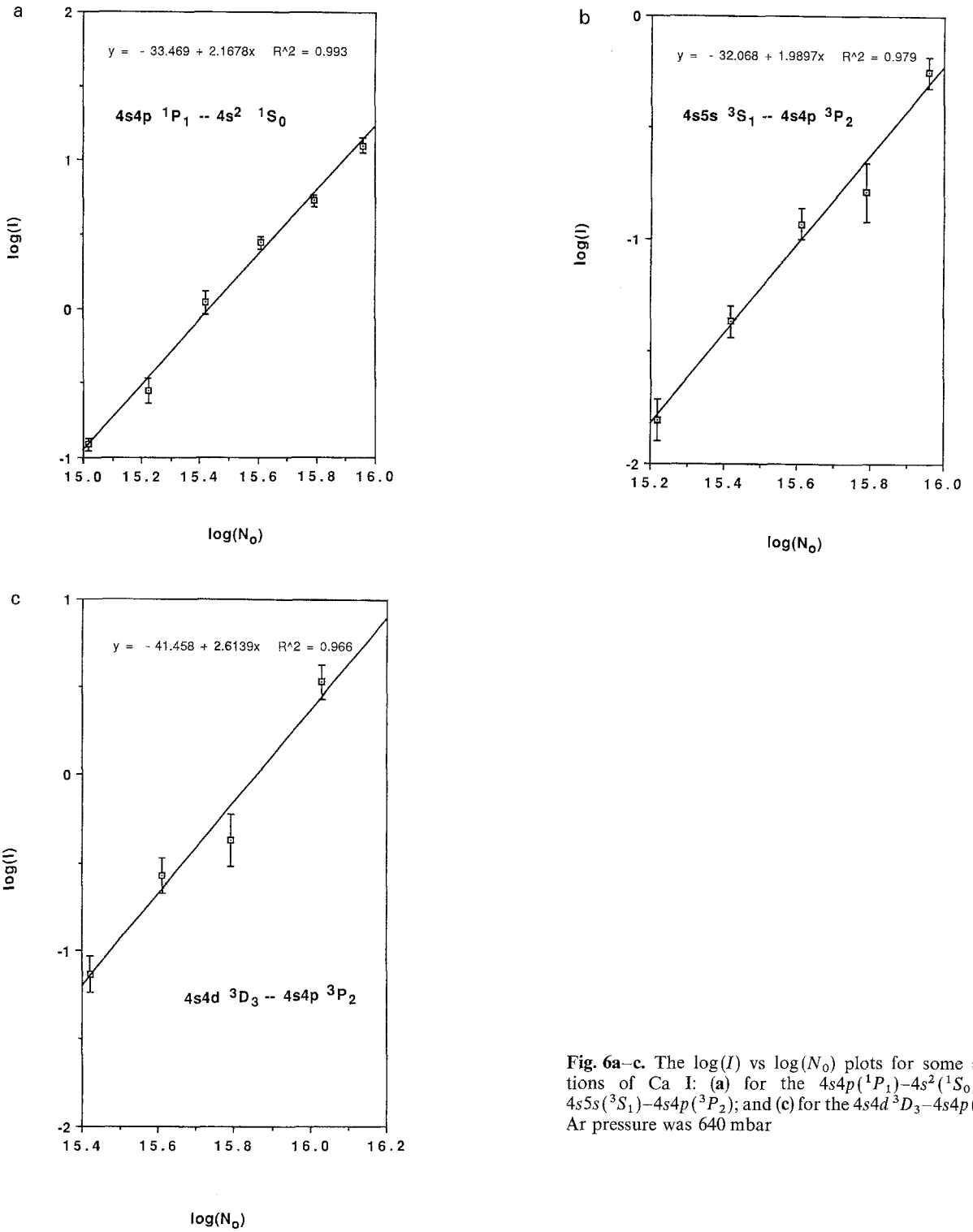

Fig. 6a–c. The $\log(I)$ vs $\log(N_0)$ plots for some selected transitions of Ca I: (**a**) for the $4s4p(^1P_1)$–$4s^2(^1S_0)$; (**b**) for the $4s5s(^3S_1)$–$4s4p(^3P_2)$; and (**c**) for the $4s4d\,^3D_3$–$4s4p(^3P_2)$. Here, the Ar pressure was 640 mbar

through

$$I = GAh\nu\beta N, \tag{10}$$

where $h\nu$ is the energy per photon, A the radiative transition probability, β the branching ratio for the detected transition and G includes the geometric factors as well as the spectral response of the photomultiplier.

Suppose that the upper state of the transition, e.g. $4s4p(^1P_1)$ or $4s5s(^3S_1)$ is populated by A–A collisions involving atoms in the $4s4p(^3P_1)$ state as in (5) and including the inherent transfer through electrons. The population N_2 of the product state thus created would be related to the population N_1 of the $4s4p(^3P_1)$ state through

$$N_2 = (k_1 N_1^2)/2, \tag{11}$$

where k_1 is the rate coefficient for the process and the factor $\frac{1}{2}$ corrects for double counting of the identical atoms.

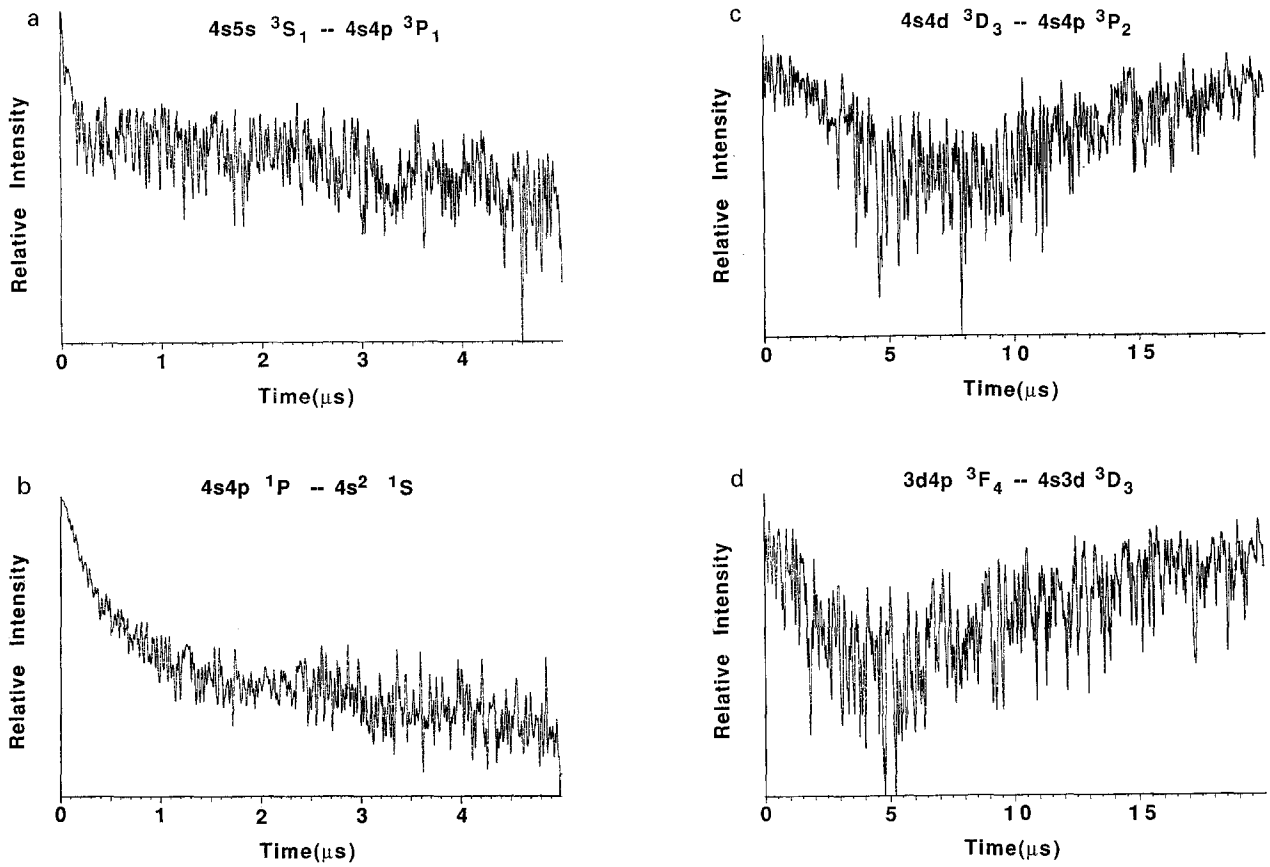

Fig. 7a–d. Typical records of time-resolved spectral emission from: (**a**) the $4s5s(^3S_1)$–$4s4p(^3P_1)$; (**b**) the $4s4p\,^1P_1$–$4s^2(^1S_0)$; (**c**) $4s4d(^3D_3)$–$4s4p(^3P_2)$; and (**d**) $3d4p(^3F_4)$–$4s3d(^3D_3)$ transitions. Here the oven temperature was 835 °C with 100 mbar Ar pressure

In the case of simultaneous or step-wise collisions of q excited atoms in the $4s4p(^3P_1)$ state (*including the energy transfer effected through electronic collisions*), the population N_p of the product state will be given by

$$N_p = (k_p N_1^q)/q. \tag{12}$$

Assuming that the laser saturates the $4s^2(^1S_0)$–$4s4p(^3P_1)$ transition, N_1 can be related to the population N_0 of the ground state through the ratio of their respective statistical weights (g_1/g_0) as below [7]:

$$N_1 = (g_1/g_0)N_0. \tag{13}$$

Combining (10), (12), and (13),

$$I_p = k'_p N_0^q, \tag{14}$$

where

$$k'_p = (GA_p h\nu\beta_p k_p)(g_1/g_0)^q/q. \tag{15}$$

Thus a graph between $\log(N_0)$ and $\log(I_p)$ should be a straight line with a slope of q.

Figure 6a–c shows the respective $\log(I)$ vs $\log(N_0)$ plots for the $4s4p(^1P_1)$–$4s^2(^1S_0)$, $4s5s(^3S_1)$–$4s4p(^3P_2)$, and $4s4d(^3D_3)$–$4s4p(^3P_2)$ transitions. The graphs are indeed linear with slopes of 2.17 (± 0.09), 1.99 (± 0.17), and 2.6 (± 0.35) respectively. The fact that these are quite close to the expected values of 2, 2 and 3 provides good support to this argument. The small deviation of the slope particularly for the third transition considered here may be due to the contributions of other atomic processes such as rapid collisional ionization of the product state, recombination into this state, or Ar-supported transfer of population to nearby states. In particular, the contribution of ionization and recombination may be significant [26, 31]. In any case, this indicates that the $4s4p(^1P_1)$ and $4s5s(^3S_1)$ states are possibly produced after one A–A collision involving $4s4p(^3P_1)$ states. However, the $4s4d(^3D_3)$ states may be produced after two A–A collisions involving three excited atoms represented, for example, by processes (5) and (7) including transfer through electrons.

2.2.2 Rate of growth of atomic population in high lying states of Ca I. In an attempt to gain some further insights into the collision dynamics of the laser-excited atoms, we have measured the rise time to the peak of spectral emission at a particular wavelength (time to reach from 10% to 90% of the peak value) through time-resolved measurements. Figure 7a, b, c and d shows, typical records of the time-resolved signals for the $4s5s(^3S_1)$–$4s4p(^3P_1)$, $4s4p(^1P_1)$–$4s^2(^1S_0)$, $4s4d(^3D_3)$–$4s4p(^3P_2)$ and $3d4p(^3F_4)$–$4s3d(^3D_3)$ transitions, respectively. Here, the oven temperature was 835 °C and Ar pressure was 100 mbar. A 50 Ω termination was again used here. However, the signal-to-noise ratio deteriorates and the fluctuations in the evolution of these states also show up. In any

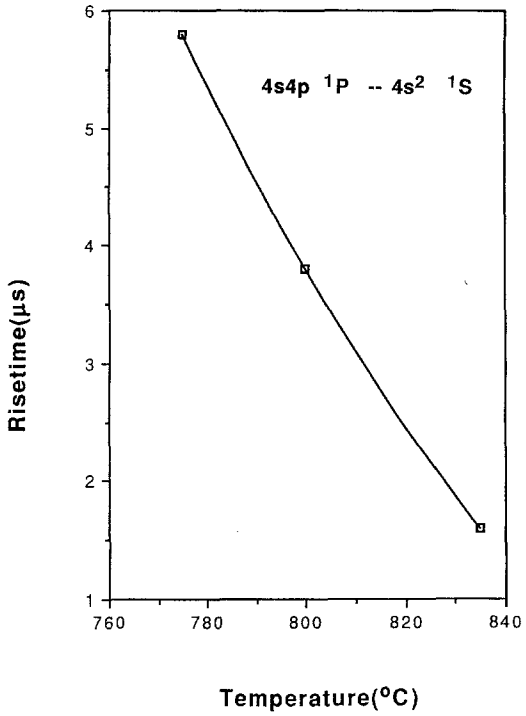

Fig. 8. Influence of oven temperature on the rise time of peak emission in the case of the $4s4p(^1P_1)$–$4s^2(^1S_0)$ transition of Ca I. Here, the Ar pressure was 28 mbar

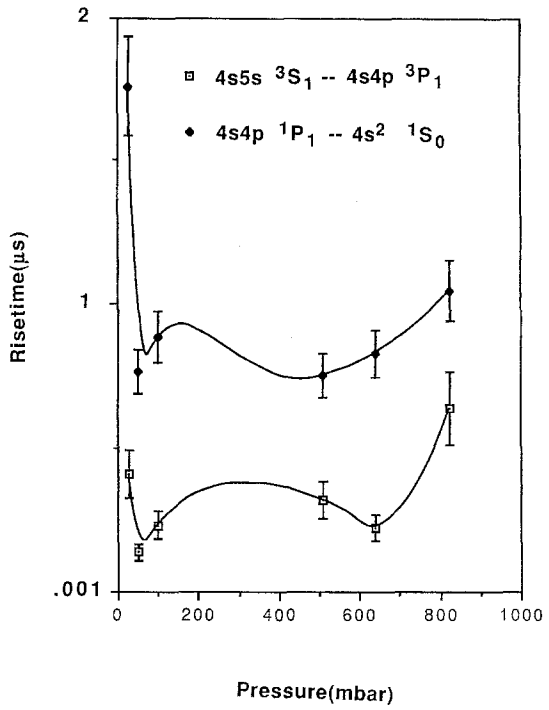

Fig. 9. Influence of Ar pressure on the rise time to the peak spectral emission: for the $4s5s(^3S_1)$–$4s4p(^3P_1)$ transition and for the $4s4p(^1P_1)$–$4s^2(^1S_0)$ transition. Here the oven temperature was 835 °C

case, some useful information may be obtained. The fact that the fastest time ≈ 0.1 μs for the peak emission is for the $4s5s\,^3S_1$ state is noteworthy. This could possibly be due to the smallest energy defect for the energy pooling collisions (Table 2). The possibility of two-photon nonlinear absorption may not be significant here because the radiation emission continues over a long period of time much beyond the laser pulse duration of 10 ns. For the $4s4p(^1P_1)$ state, the rise time is ≈ 1 μs. However, for the $4s4d(^3D_3)$ and $3d4p(^3F_4)$ states, the corresponding rise time is ≈ 3–4 μs. In a way, this supports the idea that the $4s4d(^3D)$ and $3d4p(^3F)$ states are created in two-step processes. Note that the second hump in the signals possibly indicates the onset of a new channel of population of the state under study, e.g. through recombination.

The influence of increasing oven temperature (and hence of the vapor density) on the rise time for the $4s4p(^1P_1)$–$4s^2(^1S_0)$ transition is shown in Fig. 8. The systematic decrease in the rise time is a clear indication of higher collisional rates associated with higher thermal velocities and higher densities of the excited atoms.

2.2.3 Influence of Ar on the rise time to the peak of spectral emission. We monitored the influence of increasing Ar pressure on the rise time to the peak of the spectral emission. The slowing-down of the rate of collisions with increasing Ar pressure is well understood [4]. However, the fact that Ar inhibits convective diffusion also becomes apparent here. Figure 9 sums up our results for the $4s5s(^3S_1)$–$4s4p(^3P_1)$ and $4s4p(^1P_1)$–$4s^2(^1S_0)$ transitions. At low Ar pressures (< 50 mbar), excessive convective diffusion of excited atoms in the axial direction slows down the rate of collisional energy transfer as witnessed

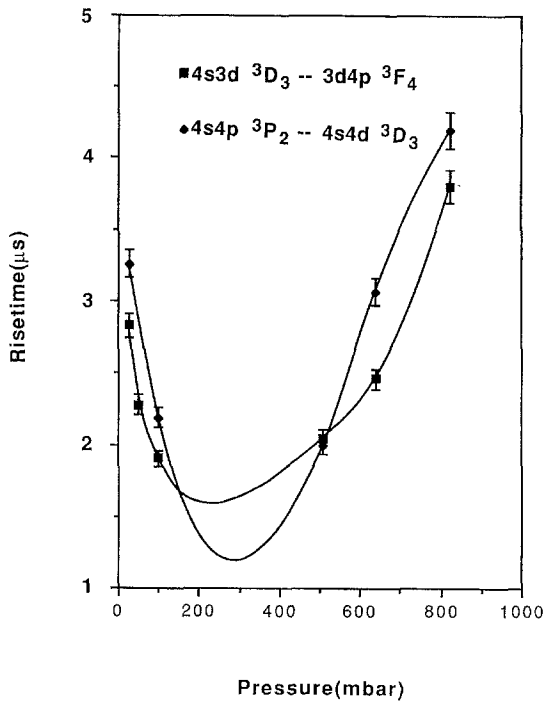

Fig. 10. Influence of Ar pressure on the rise time to the peak spectral emission: for the $4s4d(^3D_3)$–$4s4p(^3P_2)$ transition and for the $3d4p(^3F_4)$–$4s3d(^3D_3)$ transition

by the increase in the rise time to the peak emission. The rate is almost constant in the pressure range 50–650 mbar of Ar. However, at higher Ar pressures, the presence of too many Ar atoms again slows down the buildup of the

population of the upper state because the excited atoms or energetic electrons take a longer time to locate other excited atoms for the purpose of collisional energy transfer.

The results for the $4s4d(^3D_3)$–$4s4p(^3P_2)$ and the $3d4p(^3F_4)$–$4s3d(^3D_3)$ transitions are qualitatively similar (Fig. 10). The rate of increase in the rise time outside the 100–500 mbar region of Ar pressures is somewhat slower compared with the case of $4s5s(^3S_1)$–$4s4p(^3P_1)$ and $4s4p(^1P_1)$–$4s^2(^1S_0)$ transitions (Fig. 9). This would also support the possibility of two A–A collisions leading to the population of the $4s4d$ and $3d4p$ states.

3 Conclusions

Large scale collisional energy transfer among the laser-prepared Ca atoms in the $4s4p(^3P_1)$ metastable state is observed where the spectra of $4p(^2P_{3/2,1/2})$ states of Ca II were recorded for the first time in such experiments. The long radiative lifetime of the laser-prepared state [32] together with a high density of excited atoms and a collisional environment provided by high temperatures are believed to be the main factors in such a large collisional transfer. Temperature and density dependence of fluorescence intensities of some selected states together with the evolution in time of populations in various excited states provide qualitative evidence of a rapid one-step excitation of $4s5s(^3S)$ and $4s4p(^1P)$ states; and a two-step excitation of $4s4d(^3D)$ and $3d4p(^3F)$ states of Ca I.

Acknowledgements. This work is a part of Laser Research Program (Project No. 12043) supported by the Research Institute of King Fahd University of Petroleum & Minerals (KFUPM). The continuous support and encouragement from Drs. H. A. Yamani and F. F. Al-Adel is gratefully acknowledged.

References

1. B. Cheng, Z. Li, Y. Yang, J. Zhu, D. Zhang: Opt. Commun. **86**, 465 (1991)
2. M.A. Khan, E.E. Khawaja, H.A. Al-Juwair: J. Phys. B **23**, L533 (1990)
3. M.A. Khan, M.F. Al-Kuhaili: J. Phys. B **26**, 393 (1993)
4. M.A. Khan, E.E. Khawaja, M.F. Al-Kuhaili: J. Phys. D **26**, 1614 (1993)
5. M.A. Khan, E.E. Khawaja: Opt. Commun. **86**, 386 (1991)
6. P.-L. Zhang, X.-G. Wu, S.-Y. Zhao: Tech. Dig. Annual Meeting Opt. Soc. Am. (1991) Paper WE-2
7. R.M. Measures, P.G. Cardinal: Phys. Rev. A **23**, 804 (1981)
8. A. Kallenbach, M. Kock: J. Phys. B **22**, 1705 (1989)
9. K. Niemax: Appl. Phys. B **38**, 147 (1985)
10. E.E. Khawaja, M.A. Khan, H.A. Al-Juwair: Int'l J. Electron. **71**, 991 (1991)
11. D. Husain, G. Roberts: J. Chem. Soc. Faraday Trans. II **82**, 1921 (1986)
12. J.F. Kelly, M. Harris, A. Gallagher: Phys. Rev. A **38**, 1225 (1988)
13. H.G. Werij, M. Harris, J. Cooper, A. Gallagher, J.F. Kelly: Phys. Rev. A **43**, 2237 (1991)
14. D.A. Miller, L. You, J. Cooper, A. Gallagher: Phys. Rev. A **46**, 1303 (1992)
15. N. Bras, J.C. Jeannet, D. Perrin: J. Phys. B **26**, 2289 (1993)
16. P. Bicchi, C. Marinelli, E. Mariotti, M. Meucci, L. Moi: J. Phys. B **26**, 2335 (1993)
17. F. Roussel, B. Carre, P. Berger, G. Spiess: J. Phys. B **16**, 1749 (1983)
18. S. Majetich, E.M. Boczar, J.R. Wiesenfeld: J. Appl. Phys. **66**, 475 (1989)
19. J.H. Goble, W.E. Hollingsworth, J. Winn: Phys. Rev. Lett. **47**, 1881 (1981)
20. L. Barbier, M. Cheret: J. Phys. B **20**, 1229 (1987)
21. R.J. Malins, D.J. Benard: Chem. Phys. Lett. **74**, 321 (1980)
22. M.A. Khan, M.A. Gondal, M.H. Rais: Appl. Phys. B **57**, 123 (1993)
23. H.J. Yuh, P. Dagdigian: Phys. Rev. A **28**, 63 (1983)
24. W.E. Wiese, M.W. Smith, B.M. Miles, *Atomic Transition probabilities* Vol II, NSRDS-NBS 22 (US Govt. Press, Washington, DC 1969) pp. 246–254
25. M.A. Khan: KFUPM-RI Project 12043, Semi-Annual Report III (1994)
26. C.H. Skinner: J. Phys. B **13**, 55 (1980)
27. J.L. Le Gouet, J.L. Picque, F. Wuilleumier, J.M. Bizau, P. Dhez, P. Koch, D.L. Ederer: Phys. Rev. Lett. **48**, 600 (1982)
28. J. Sugar, C. Corliss: J. Phys. Chem. Ref. Data **14**, Suppl. 2, 51 (1985)
29. M.A. Khan, M.A. Gondal, M.H. Rais: J. Phys. B **27**, 2889 (1994)
30. M.A. Khan, J.-P. Connerade, M. Rafique: J. Phys. B **27**, L563 (1994)
31. A. Burgess, H.P. Summers: Astrophys. J. **157**, 1007 (1969)
32. P.S. Furcinitti, L.C. Balling, J.J. Wright: Phys. Lett. A **53**, 75 (1975)